



Dissociation energies of silver clusters

Ag_n^+ , $n = 14, 15, 16, 18$

Klavs Hansen^{a,1}, Alexander Herlert^b, Lutz Schweikhard^{c,*}, Manuel Vogel^b

^a Department of Physics, University of Jyväskylä, P.O. Box 35, FIN-40014 Jyväskylä, Finland

^b Institut für Physik, Johannes Gutenberg-Universität, D-55099 Mainz, Germany

^c Institut für Physik, Ernst-Moritz-Arndt-Universität, D-17487 Greifswald, Germany

Received 14 October 2002; accepted 11 November 2002

Abstract

A recently developed method to determine dissociation energies has been applied to positively charged silver clusters of size $n = 14, 15, 16$ and 18 . The method uses a combination of sequential and single step decays. It requires an uncalibrated thermometer which here is provided by the evaporation rate constants of the product clusters. For this purpose, earlier measurements [J. Chem. Phys. 57 (1998) 2786] are reanalyzed with the new method. The resulting dissociation energies are compared with the liquid drop values and the measured decay rate constants with expected rate constants from detailed balance theory.

© 2003 Elsevier Science B.V. All rights reserved.

Keywords: Dissociation energies; Silver clusters; Ag_n^+

1. Introduction

Chemical reaction studies and the determination of the stability of molecules in general has been one of the major undertakings of chemical physics in the last century. In the field of clusters, the importance of energetics and stabilities has been amply illustrated by the discovery of shell structure in the form of electronic shell structure and geometric packing of atoms [1–3]. Other manifestations of stability related phenomena have been found, such as the odd–even effect

in metal clusters and shape deformations in clusters of simple metals.

These effects were discovered in molecular beams and, with few exceptions, have retained their strongest expression for free particles in high vacuum. This fact causes some difficulties in the measurements of the precise magnitude of the effects. One fundamental question is the total binding energy of the free clusters or, as a somewhat simpler and experimentally more accessible quantity, the difference between the total binding energies of two clusters which differ in size by a single atom or two. However, absolute energies or even energy differences are not easily measured. As a consequence, a number of investigations have been concerned with the relation between the separation energy, i.e., the energy needed to separate an atom (or a small group of atoms) asymptotically far

* Corresponding author.

E-mail address: lutz.schweikhard@physik.uni-greifswald.de (L. Schweikhard).

¹ Present address: Department of Experimental Physics, Göteborg University and Chalmers University of Technology, SE-41296 Göteborg, Sweden.

from a cluster and the corresponding rate constants, which can be accessed experimentally.

In practice, the experiments are often performed as photoexcitation studies where one or more photons with a well defined energy are absorbed by the cluster and the subsequent unimolecular decay is observed time-resolved. The modeling of the experimental rates in terms of the dissociation energies usually requires some assumptions, mainly about the thermal property of the cluster, precursor and product alike. Experiments of this type on small and medium size singly charged silver cluster cations were reported in [4]. Dissociation energies were extracted from an analysis where QRRK (Quantum–Rice–Ramsperger–Kassel) theory was used to model the time dependence of the decay (see references in [4]). We now believe that the QRRK theory is far from sufficient for this analysis.

As an alternative to photoexcitation one can use collision-induced dissociation (CID). Such an investigation is reported in [5] for singly charged silver clusters of a somewhat larger size range as in the photoexperiments. In addition to the QRRK used in the photoexcitation experiments, the analysis requires that the energy transfer is modeled. The resulting values are surprisingly close to those found by the present study (see below), which testifies to the quality of the energy transfer function used in the analysis, although some amount of accidental error cancellation may also have occurred.

Irrespective of whether photoexcitation or CID is used, one is faced with the fact that in a realistic description the evaporation rate depends on the activation energy for the process, on the excitation energy and on the level densities of the precursor and product cluster. The latter are frequently unknown and one has to make an educated guess about the functions. In some experiments, the cluster temperature has been set by thermalization to a heat bath, which converts the problem to the measurement of decay rate constants vs. temperature and relying on an Arrhenius plot [6]. In another series of experiments, the heat bath method was combined with photoexcitation to yield caloric curves ($E(T)$) for sodium clusters. This should reduce the amount of modeling required

to extract dissociation energies from rate constants substantially [7]. Unfortunately, in general, the application of a heat bath is not easily accomplished.

In addition to the lack of knowledge of the caloric curves, radiative cooling may play an important role for the apparent, i.e., measured, unimolecular decay-rate constants. Radiative cooling is often only manifested indirectly in an experiment via the influence it has on the rate constants. It can easily occur undetected since it is non-destructive in the sense that neither the mass nor the charge of the cluster is changed by photon emission. Dedicated experiments have amply demonstrated the importance of emission of thermal IR radiation in the decay dynamics of molecules and molecular clusters. In particular, Dunbar and co-workers have performed several investigations: for example, a pump-probe technique was applied and the amount of radiation inferred from the temporal behavior of a molecular disintegration ratio [8]; radiation was also inferred by its effect on the excitation energy dependence of a unimolecular reaction [9].

Fullerenes and clusters of refractory metals have been shown to cool by thermal radiation, too [10–13]. The fullerenes are a point in case: the effect of radiative cooling, although strong even on the time scale of time-of-flight mass spectrometers, was only observed a decade after the discovery of the molecules and after a large number of experimental results on their unimolecular decay had been published.

From the discussion given above, it is obvious that even though the theories of unimolecular decays and their rates are relatively simple, the amount of work required to actually apply them can be quite extensive. Thus, alternative, less tedious methods are highly desired.

Recently, a number of these problems have been circumvented by a method designed to measure the dissociation energies of molecules and clusters as directly as possible [14]. The method has been reviewed and extended in a number of publications [15–18] and thus only a short sketch is presented: in the simplest version, which will be used here, one measures the energy dependence of the rate constant of the last decay

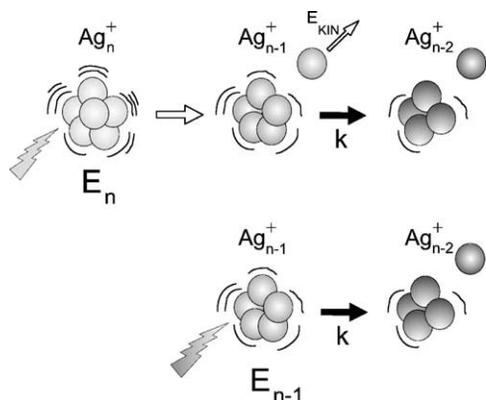


Fig. 1. Schematics of the model-free determination of the dissociation energy in case of silver cluster cations.

in two decay chains of different length (Fig. 1). When the excitation energy of the two different chains is adjusted to give the same rate constants of the observed decay, the energy consumed in the first decay(s) of the longer chain is identical to the difference between the excitation energy of the longer and the shorter chain. Apart from minor corrections, this energy difference is the dissociation energy. The decay rate of the shorter chain acts, in effect, as an uncalibrated thermometer, somewhat analogous to the use of the unimolecular decay to detect radiation in [8].

In the following, we analyze data on the decay rate constants of cationic silver clusters [4] by this method. Measured rate constants for the direct decay $\text{Ag}_{n-1}^+ \rightarrow \text{Ag}_{n-2}^+$ are compared with the rate constants for the last step in the decay chain $\text{Ag}_n^+ \rightarrow \text{Ag}_{n-1}^+ \rightarrow \text{Ag}_{n-2}^+$ (Fig. 1) for the cluster sizes $n = 14, 16$ and 18 . At identical measured rate constants for the two decays, the dissociation energy, defined as $D_n = -(E_n - E_{n-1}) + E_1$, where E_n is the ground state energy of cluster size n , is [14]

$$D_n = E_{\text{ph},n} - E_{\text{ph},n-1} + E_{\text{th},n} - E_{\text{th},n-1} - E_{\text{KER}}, \quad (1.1)$$

where subscripts th indicate room temperature thermal energies, ph photoexcitation energies and KER the kinetic energy release [19]. The quantities E_{KER} and $E_{\text{th},n}$ are average values. In the case of Ag_{15}^+ a

multisequential decay chain is compared to a sequential process and the direct decay of Ag_{13}^+ . A multisequential decay chain is one which consists of at least three decays, i.e., $A \rightarrow B \rightarrow C \rightarrow D$.

2. Experimental procedure and results

The experiments have been described in full detail by Hild et al. ([4] and references therein). Briefly, the clusters are produced in a laser vaporization source, cooled by a helium gas pulse, and transferred to the Penning trap where they are captured by gating entrance and exit electric potentials. In the trap they are size-selected by radial ejection of all unwanted cluster ions. Thermalization to room temperature is accomplished by collisions with argon gas that is pulsed into the trap region. Experiments on gold clusters show that already the helium gas in the source provides most of the thermalization of the clusters right after the production [14]. After size selection, the clusters are exposed to the light from the excitation laser, a pulsed (10 ns) frequency-doubled dye laser, pumped by the second or third harmonic of a Nd:YAG laser. After photoexcitation, the temporal development of the decay is followed by delayed ejection of the trapped ions into a time-of-flight mass spectrometer. All charged particles, precursors and products alike, are detected in a conversion-electrode detector. The mass spectrometer is linear, i.e., without reflectron. The clusters that decay during the flight from the trap to the detector will be detected as the parent size and the flight time in the spectrometer is therefore irrelevant. Hence, the storage time and the delay time is the same, up to the very small ambiguity of the transit time through the acceleration stage of the mass spectrometer.

Each delay time between laser pulse and time-of-flight measurement gives one corresponding point on the decay curve. Changing the delay between the laser pulse and the extraction provides the time dependence from which the decay rate constant is fitted. The decay is found to be exponential over the time range investigated which signals a statistical decay with a single decay constant. As an example, the relative abundances

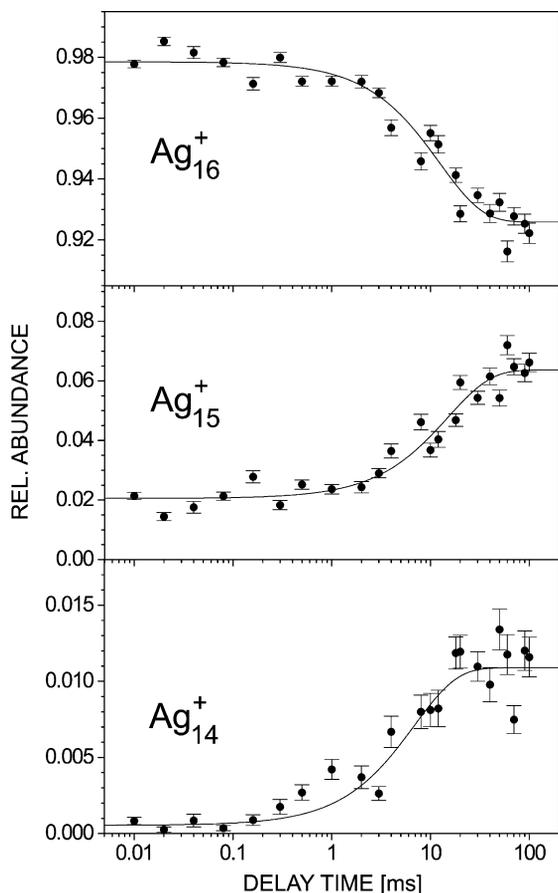


Fig. 2. Relative abundance of silver clusters Ag_n^+ , $n = 14, 15$ and 16 , as a function of the delay time between photoexcitation of Ag_{16}^+ ($h\nu = 2.96 \text{ eV}$) and ejection for TOF mass analysis. The lines are exponential fits.

of Ag_n^+ , $n = 14\text{--}16$, after photoexcitation of Ag_{16}^+ ($h\nu = 2.96 \text{ eV}$) are shown as a function of the delay time in Fig. 2. For $n = 16$, an exponential decay is observed (note that the time scale in the figure is logarithmic). Those clusters that have absorbed one photon evaporate a single monomer which shows as an exponential buildup for $n = 15$. However, a small fraction of the initial cluster ions has absorbed two photons which leads to a sequential decay to Ag_{14}^+ . For the analysis, only the buildup time constant for $n = 14$ ($\tau = (6.2 \pm 1.5) \text{ ms}$) is relevant, since it is equal to the decay-time constant of Ag_{15}^+ . In the following, it

is compared to the time constant as observed in the direct decay, i.e., upon excitation of size-selected Ag_{15}^+ clusters.²

All sizes examined in the present study, except Ag_{13}^+ , evaporate neutral monomers [20,21]. The cluster size $n = 13$ has a finite branching ratio between monomer and dimer evaporation. Within the uncertainties, the time constants for appearance of $n = 12$ and $n = 11$ are consistent with the disappearance of $n = 13$ and either values can be used for the analysis. The present study is limited to a small number of points on each curve of k vs. photoexcitation energy. This excludes the rigorous experimental checks on the validity of the method applied in [14]. However, the situation is very similar to the well-documented case of gold clusters and we will analyze the data with the experience of the higher statistics of gold clusters.

The measured decay-time constants from [4] that are analyzed with the new method are listed in Table 1. For the direct decays $\text{Ag}_n^+ \rightarrow \text{Ag}_{n-1}^+$ an average time constant has been calculated from the decay of the precursor cluster size n and the buildup of the product cluster size $n - 1$. The fit of the time constants come with fitted uncertainties, σ_i ($i = 1, 2$). The difference in the decay and the buildup rate constants appear to be a little higher than can be explained by the fitted uncertainties. The reason for this is not clear. The average and the uncertainty is calculated as

$$\bar{\tau} = \frac{w_1 \tau_1 + w_2 \tau_2}{w_1 + w_2},$$

$$\sigma^2 = \frac{w_1 (\tau_1 - \bar{\tau})^2 + w_2 (\tau_2 - \bar{\tau})^2}{w_1 + w_2}, \quad (2.1)$$

where the weights are $w_i = 1/\sigma_i^2$. Uncertainties quoted will always be 1σ .

The corresponding decay rates, i.e., the inverse of the decay-time constants, are plotted as a function of the photoexcitation energy in Fig. 3. The cases (a) (left), (b) and (c) show the comparison of the sequential decay to a single decay step for the determination

² The single-step decay of Ag_{16}^+ to Ag_{15}^+ is not used for the determination of dissociation energies in the present study. It would have to be combined with the sequential decay of Ag_{17}^+ in order to determine the dissociation energy of Ag_{17}^+ .

Table 1

Constants τ for the direct decays and for the last step of the sequential and multisequential decays of size-selected silver clusters Ag_n^+ after photoexcitation with energy E_{ph} (from [4])

Process	n	E_{ph} (eV)	τ_n (ms)	τ_{n-1} (ms)	τ (ms)
Direct	13	3.44	5.0 ± 1.1	3.6 ± 0.6	3.9 ± 0.6
		3.73	0.30 ± 0.06	0.26 ± 0.05	0.28 ± 0.04
	15	3.72	5.8 ± 2.9	10.7 ± 1.5	9.7 ± 2.0
		4.00	13.5 ± 6.2	3.4 ± 0.7	3.5 ± 1.1
	17	2×2.28	2.5 ± 0.9	1.2 ± 0.3	1.3 ± 0.4
Sequential	14	2×2.76			1.2 ± 0.3
		2×2.88			0.23 ± 0.08
	16	2×2.96			6.2 ± 1.5
		2×3.12			2.0 ± 0.4
18	3×2.28			1.9 ± 0.5	
Multisequential	15	2×4.00			2.8 ± 0.8

In case of the direct decays, the mean value for τ is calculated from the decay of the precursor cluster size n (τ_n) and from the formation of the product cluster size $n - 1$ (τ_{n-1}).

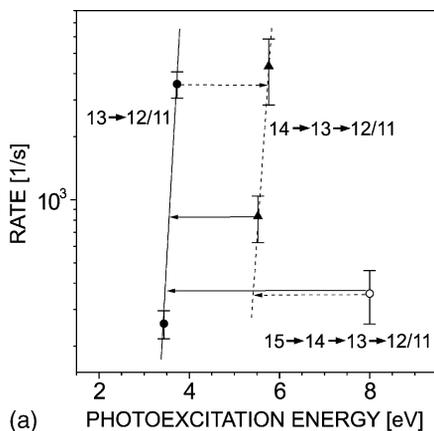
of the dissociation energies D_{14} , D_{16} and D_{18} , respectively. In (a), indicated at the bottom, the multisequential decay of Ag_{15}^+ is compared to the sequential decay of Ag_{14}^+ .

Both the energetic shifts and their uncertainties must be estimated differently from the procedure given in [16] because the determination of the shape of curve describing the rate constants vs. photoexcitation energy would not be reliable. As an alternative, we use a linear interpolation of the logarithm of the rate constant vs. photoexcitation energy. For $n = 14$, this permits an interpolation in two cases (left solid and dashed arrows in Fig. 3(a)), and yields values for the shift of $\Delta E_{\text{ph}} = 1.95(4)$ and $2.01(8)$ eV, respectively. The shift, ΔE_{ph} is defined as the difference in photoexcitation which gives the same rate constant for the last, observed decay. The procedure for estimating the uncertainty of the energy shifts is described in Fig. 4: the error bars of the rate of the sequential decay are projected onto the lines connecting the error bars of the direct decay rates. The minimal and maximal energies are read off the energy-axis to determine the shift and its uncertainty. The two values of the energy shift are combined by calculation of the weighted average: $\Delta E_{\text{ph}} = 1.96(4)$ eV. Similarly, for $n = 16$, two values for the energy shift are found: $2.06(15)$ and $2.07(16)$ eV, which yield $\Delta E_{\text{ph}} = 2.06(11)$ eV for

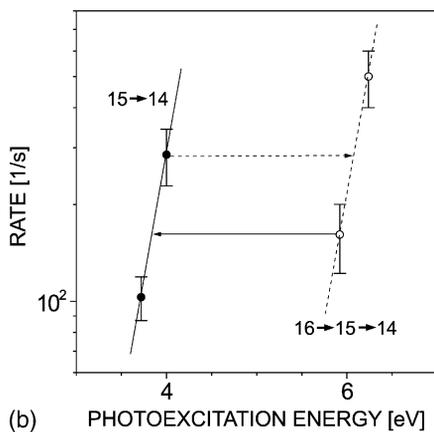
the mean value. For $n = 15$, there is only one point which has to be projected onto the extrapolated line of the sequential decay of Ag_{14}^+ . Thus, the resulting uncertainty is larger than in the cases examined above: $\Delta E_{\text{ph}} = 2.67(16)$ eV. Finally, the energy shift is determined for $n = 18$, where only one point each for the direct and the sequential decay is available. In order to give a conservative estimate of the uncertainty, the smallest slope of this investigation (which results in the largest values of the uncertainty) is taken, i.e., the linear interpolation of the case $n = 16$ (Fig. 3(b)). Thus, the energy shift is determined as $\Delta E_{\text{ph}} = 2.45(27)$ eV.

The room temperature thermal energies, E_{th} , which enter as a difference, $E_{\text{th},n+1} - E_{\text{th},n}$, are calculated by extrapolation of the bulk values per vibrational degree of freedom (0.02 eV) with the number of vibrational degrees of freedom in the cluster. Since the bulk heat capacity at room temperature is close to that of a Debye crystal we expect that the error is very small.

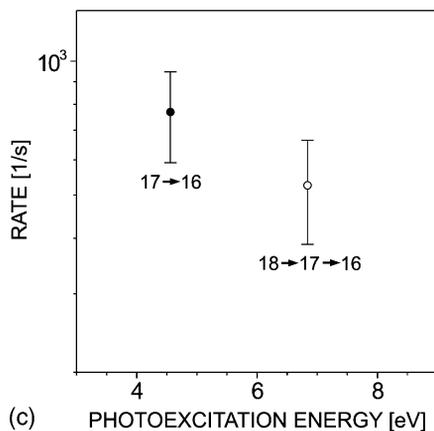
The kinetic energy release is calculated with the procedure given in [16]. The kinetic energy is a stochastic quantity and the distribution has a mean and width comparable to the microcanonical temperature of the product cluster, in our case the temperature of the cluster of the thermometer process. It is calculated from the detailed balance equation [22] (given



(a) PHOTOEXCITATION ENERGY [eV]



(b) PHOTOEXCITATION ENERGY [eV]



(c) PHOTOEXCITATION ENERGY [eV]

Fig. 3. Rates for the direct, sequential and multisequential decays of silver cluster cations Ag_n^+ (data from [4]). The rates for direct decays are averaged values (see Table 1 and text). The solid and dashed lines indicate the method of linear interpolation and projection (for details see Fig. 4).

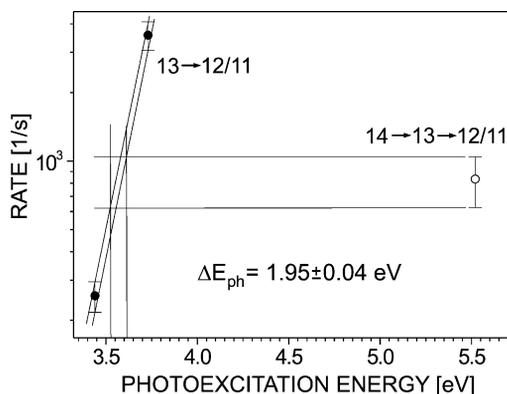


Fig. 4. Estimation of the uncertainty of the energy shift in case of the projection of the rate from the sequential process $\text{Ag}_{14}^+ \rightarrow \text{Ag}_{13}^+ \rightarrow \text{Ag}_{11,12}^+$ onto the linear interpolation for the direct decay $\text{Ag}_{13}^+ \rightarrow \text{Ag}_{11,12}^+$.

below as Eq. (3.1)). It requires the microcanonical temperature, T_m [23] and the capture cross section for the inverse process. The latter is found by assuming that the incoming atom moves in a classical potential given by the charge of the cluster and the polarizability of the silver atom, 7.9 \AA^3 ,³ and that the atom sticks when it touches the cluster with a geometric cross section of $\sigma_{\text{geo}} = \pi r_1^2 ((n-1)^{1/3} + 1)^2$. The room temperature value of the Wigner–Seitz radius is used, $r_1 = 1.60 \text{ \AA}$ [24]. This cross section assumes no reverse activation barrier, i.e., that the separation energy is equal to the activation energy for the thermal process. The resulting KER values are close to $2k_B T_m$, which reflects the fact that the interaction energy due to the polarizability is small. As in the case of the room temperature thermal energy, the microcanonical temperature, T_m , is estimated from the bulk caloric curve per atom with an effective number of atoms reduced to $n-2$ to account for the six translational and rotational degrees of freedom. The values are $k_B T_m = 0.12\text{--}0.13 \text{ eV}$, except for $n=15$ where it is $k_B T_m = 0.17 \text{ eV}$. Note, that the relevant temperatures are those of the product clusters. Only for the multisequential decay of $n=15$ does the scaling from bulk values cause a problem since the temperature of the

³ Literature values differ and we have used an average.

Table 2

Model-free dissociation energies D_n of silver cluster cations Ag_n^+ calculated from the energy shift ΔE_{ph} , the difference in the thermal energy ΔE_{th} , and the kinetic energy release E_{KER} for the evaporated atom (uncertainties given in parenthesis)

n	ΔE_{ph} (eV)	ΔE_{th} (eV)	E_{KER} (eV)	D_n (eV)
14	1.96(4)	0.06	0.20(4)	1.82(6)
15 ^a	2.67(16)	0.06	0.26(5)	2.47(17)
15 ^b	4.52(5)	2×0.06	$0.26(5) + 0.20(4)$	2.36(10)
16	2.06(11)	0.06	0.19(4)	1.93(12)
18	2.45(27)	0.06	0.20(4)	2.31(27)

^a Multisequential decay compared to sequential decay.

^b Two subsequent decays; for the determination of D_{15} the model-free dissociation energy $D_{14} = 1.82(6)$ is applied.

first product is significantly above the bulk melting temperature. We have used a linear extrapolation of the bulk heat capacities from the melting point in this case. The KER values and the resulting dissociation energies are listed in Table 2 and the dissociation energies are plotted in Fig. 5. The statistical and systematic uncertainties have been added in square.

A comment on the value of the KER may be in place. In chemical literature a frequently calculated value is that of $k_{\text{B}}T_{\text{m}}$ instead of the almost $2k_{\text{B}}T_{\text{m}}$ here. A value of $2k_{\text{B}}T_{\text{m}}$ results from the situation where in the reverse process of atom capture absorp-

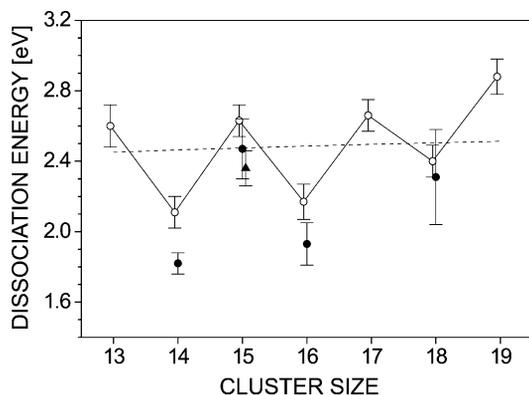


Fig. 5. Dissociation energies as a function of cluster size. Full circles: model-free method. Full triangle: multisequential vs. direct decay. Open circles: QRRK values (from [4]). Dashed line: liquid drop model.

tion happens with a cross section which is independent of the kinetic energy of the atom. This follows from kinetic gas theory [25] and was first applied to clusters by Engelking [26]. One important example of this kind of cross sections is the geometric cross section. With the exception of zinc, all bulk metals have this cross section and to our knowledge no experiment has shown any sign of a reverse activation barrier for evaporation of a neutral atom from any metal cluster.

For $n = 15$, the multisequential decay can also be compared to the direct decay of Ag_{13}^+ , where two consecutive decay steps enter the calculation: the decay of Ag_{15}^+ , with an unknown dissociation energy, and the decay of Ag_{14}^+ , where the previously determined value $D_{14} = 1.82(6)$ eV can be included in the analysis. The energy shift is shown in Fig. 3(a). In contrast to the multisequential/sequential comparison, no extrapolation of rate constants vs. excitation energy is necessary and the shift of the multisequential data point to the interpolated line is $\Delta E_{\text{ph}} = 4.52(5)$ eV. In order to extract the dissociation energy of $n = 15$, both KERs, $E_{\text{KER},15}$ and $E_{\text{KER},14}$, the dissociation energy D_{14} , and twice the thermal energy difference $E_{\text{th}} = 0.06$ eV enter as terms. The result for the dissociation energy is $D_{15} = 2.36(10)$ eV. It agrees well with the value found by comparison of multisequential and sequential decay and has a smaller uncertainty.

The model-free values are systematically lower than the QRRK values [4] by 5–13%. This deviation is of similar magnitude as the one encountered for Au_n^+ [14] but of opposite sign.

It is interesting to compare the measured values of the dissociation energies with those resulting from the liquid drop model, i.e., an extrapolation from the bulk values (see Fig. 5):

$$D_{\text{ld}} = D_{\infty} - \frac{8\pi}{3} n^{-1/3} r_1^2 \sigma_{\text{surf}}. \quad (2.2)$$

where σ_{surf} is the surface tension. (For the present study, the contribution of the Coulomb term can be neglected.) We have used the zero-K value $D_{\infty} = 2.966$ eV [27] and the melting point value $\sigma_{\text{surf}} =$

0.91 J/m² [28]. Hence,

$$D_{\text{ld}} = 2.97 - \frac{1.22 \text{ eV}}{n^{1/3}}. \quad (2.3)$$

The dashed line in Fig. 5 indicates D_{ld} as a function of cluster size.

When comparing the measured values with the liquid drop values, it should be kept in mind that the latter do not incorporate the odd–even effects. The even-numbered clusters (here $n = 14, 16$ and 18) contain an odd number of valence electrons and are therefore less stable than the average, whereas for the odd cluster size $n = 15$, the trend is expected to be reversed. For gold clusters the odd–even effect is approximately 10% of the total dissociation energy in the size range $n = 10$ – 20 . The present results for silver suggest an odd–even effect of about 20% and a mean dissociation energy which is 10–20% below the liquid drop value. For the comparison of the measured values with the liquid drop model values several points are relevant. First of all, the uncertainty in the measured bulk surface tension is finite. In addition, the parameters of the liquid drop model are extrapolated by about 20 orders of magnitude and terms of lower order in $n^{1/3}$ have not been included.

3. Discussion

The measured rate constants were used to extract the dissociation energies via the QRRK formula in [4]. It was assumed that the level density was that of an Einstein crystal. As already mentioned, the resulting values are consistently higher than the ones derived from the present and much improved analysis of the same data (see Fig. 5). Apart from the problems with QRRK, a possible explanation of the systematics is that the assumption of the cluster as an Einstein crystal is invalid. Whereas the bulk value of the room temperature thermal properties conform well to that of a Debye crystal, the heat capacity of the bulk is significantly higher than the $3k_{\text{B}}$ per atom for harmonic oscillators at the elevated temperatures where unimolecular decay takes place. This effect, if applicable to clusters,

reduces the effective temperature for a given excitation energy. If we disregard the frequency factors in the expressions for the rate constants, this requires a reduced value of the dissociation energy to yield the same rate constants. Hence, the lower value of the dissociation energy is consistent with a heat capacity which is higher than the one for harmonic oscillators.

A calculation of the rate constants with Frauendorf's application of the Weisskopf formula to clusters [22] also indicates that the heat capacities are underestimated, even compared with the bulk values. The rate constant used is based on the detailed balance, or Weisskopf, formula for monomer evaporation from cluster size n :

$$k_n(E) d\epsilon = \frac{gm\sigma(\epsilon)}{\pi^2\hbar^3} \epsilon \frac{\rho_{n-1}(E - D_n - \epsilon)}{\rho_n(E)} d\epsilon, \quad (3.1)$$

where E is the excitation energy, g is the spin degeneracy of the evaporated atom ($=2$ for silver), m is the reduced mass of the channel (close to the mass of the silver atom in our case), σ is the atom capture cross section for the inverse process, the ρ 's the level densities of the clusters, D_n the dissociation energy, and ϵ the translational kinetic energy of the channel, basically that of the evaporated silver atom.

As argued above, the cross section can be assumed to be close to the geometric value for the purpose of calculating rate constants although, that this approximation is not sufficiently precise for the calculation of the kinetic energy release. The kinetic energy release can be integrated out to give T^2 . The only remaining unknown are then the level densities. They were approximated by the values extrapolated from bulk thermal properties. The resulting formula reads

$$k_n(E) = \frac{gmR^2}{\pi\hbar^3} T_n(E) T_{n-1}(E - D_n) \times \sqrt{\frac{C_n(E)}{C_{n-1}(E - D_n)}} e^{S_{n-1}(E - D_n) - S_n(E)}. \quad (3.2)$$

Here T_n is the temperature, C_n the heat capacity and S_n the entropy of the cluster of size n . The argument refers to the energy content and the values are found from the bulk curve, scaled with the excitation energy per atom.

The rate constants calculated with Eq. (3.2) are consistently higher than the measured values (see reference [4]). The number of photons assigned are one for $n = 14, 15, 16$, and two for $n = 18$. Other assignments give much larger discrepancies. For $n = 14$, the factors are 710 and 970 at the two measured energies, for $n = 15$, the numbers are 70 and 170, for $n = 16$, they are 160 and 260 and for the single point for $n = 18$ it is 25. For $n = 14, 15$ and 16, the high value is for the highest photon energy. It corresponds to a microcanonical temperature which is from 160 K (for $n = 14$) to 95 K ($n = 18$) too high in the calculations. The theoretical curve can be brought in rough (albeit not perfect) agreement with the measured rate constants if one arbitrarily increases the heat capacity with an overall factor on the extrapolated bulk values. The scaling factor is between 1.1 and 1.2 which does not seem an unlikely value, in particular since melting has not been taken into account in the extrapolation from bulk values. One may speculate that a weak and smeared solid–liquid like transition could cause a slight increase in the heat capacity. The melting point of even larger silver clusters is in fact measured to be reduced to 40% of the bulk value [29]. We stress the tentative nature of this conclusion.

Some quantum mechanical calculations beyond the jellium approximation [30] have been reported in the literature for silver clusters above size 10. A number of structure optimizations based on tight binding calculations or empirical potentials have appeared in the literature but unfortunately do not calculate what we measure which makes a comparison between experiment and theory difficult [31–35].

A comparison with experimental data on electron affinities and ionization energies is limited to the magnitude of the odd–even effect which, even if it hinges on a single odd–even–odd ($n = 14$ –15–16) sequence, is more interesting. In the jellium model the odd–even variations in electron affinities, dissociation energies and ionization energies (a.k.a. ionization potentials) are identical in the lowest approximation. The IE's of $n = 13$ –15 from [36] show a peak-to-peak amplitude of the odd–even effect of 0.3 eV, compared with the analogous magnitude for the dissociation energies of

0.50 ± 0.13 eV. The amplitude observed in photoionization experiments amounts to 0.5 eV, i.e., the same value as for the dissociation energies [37]. The electron affinities (EA) deviate to the high side. The amplitude for $n = 12$ –14 is 0.76 eV [38] and 0.7 eV [39] (the $n = 13$ value of [38] was reassigned by us since the first peak in the measured electron energy spectrum is very weak). Although these two values are marginally consistent with our result, the difference between the IE value and the EA seems to be real and can probably be ascribed to a breakdown of the jellium picture. In this connection, it is of interest to note that for smaller ($n \leq 11$) anionic silver clusters the odd–even staggering in electron affinities and in the dissociation energies are very close [40]. Even if the dissociation energies are not model-free, a scaling with typically 10% as between the Hild et al. data and the model-free analysis here will not change the good agreement.

4. Conclusion

We have reanalyzed earlier experimental results with a recently developed method to determine the dissociation energies of the silver cluster cations Ag_n^+ , $n = 14, 15, 16$ and 18. The new results are shifted by 5–13% below the previous values based on a QRRK evaluation of decay rate constants. A comparison with calculated rate constants shows the strength of the new method: Instead of extracting dissociation energies from rate equations and a number of assumptions, knowledge of the dissociation energy and the measured rate constants now allows one to test the remaining input parameters and assumptions, as e.g., the parametrization of the level densities. The importance of the method and results presented here therefore reaches beyond the mere determination of dissociation energies.

Acknowledgements

This work has been supported by the DFG, the EU network “CLUSTER COOLING” and the Academy

of Finland under the Finnish Center of Excellence Programme 2000–2005 with a grant to K.H.

References

- [1] O. Echt, K. Sattler, E. Recknagel, *Phys. Rev. Lett.* 47 (1981) 1121.
- [2] W.D. Knight, K. Clemenger, W.A. de Heer, W.A. Saunders, M.Y. Chou, M.L. Cohen, *Phys. Rev. Lett.* 52 (1984) 2141.
- [3] T.P. Martin, T. Bergmann, H. Gölich, T. Lange, *Chem. Phys. Lett.* 172 (1990) 209.
- [4] U. Hild, G. Dietrich, S. Krückeberg, M. Lindinger, K. Lützenkirchen, L. Schweikhard, C. Walther, J. Ziegler, *J. Chem. Phys.* 57 (1998) 2786.
- [5] S. Krückeberg, G. Dietrich, K. Lützenkirchen, L. Schweikhard, C. Walther, J. Ziegler, *J. Chem. Phys.* 110 (1999) 7216.
- [6] J. Borggreen, K. Hansen, F. Chandezon, T. Døssing, M. Elhajal, O. Echt, *Phys. Rev. A* 62 (2000) 013202.
- [7] M. Schmidt, R. Kusche, W. Kronmüller, B. von Issendorff, H. Haberland, *Phys. Rev. Lett.* 79 (1997) 99.
- [8] G.T. Uechi, R.C. Dunbar, *J. Chem. Phys.* 93 (1990) 1626.
- [9] R.C. Dunbar, C. Lifshitz, *J. Chem. Phys.* 94 (1994) 3542.
- [10] K. Hansen, E.E.B. Campbell, *J. Chem. Phys.* 104 (1996) 5012.
- [11] C. Walther, G. Dietrich, W. Dostal, K. Hansen, S. Krückeberg, K. Lützenkirchen, L. Schweikhard, *Phys. Rev. Lett.* 83 (1999) 3816.
- [12] R. Mitzner, E.E.B. Campbell, *J. Chem. Phys.* 103 (1995) 2445.
- [13] U. Frenzel, A. Roggenkamp, D. Kreisler, *Chem. Phys. Lett.* 240 (1995) 109.
- [14] M. Vogel, K. Hansen, A. Herlert, L. Schweikhard, *Phys. Rev. Lett.* 87 (2001) 013401.
- [15] M. Vogel, K. Hansen, A. Herlert, L. Schweikhard, *Chem. Phys. Lett.* 346 (2001) 117.
- [16] M. Vogel, K. Hansen, A. Herlert, L. Schweikhard, *Phys. Rev. A* 66 (2002) 033201.
- [17] M. Vogel, K. Hansen, A. Herlert, L. Schweikhard, *Eur. Phys. J. D* 21 (2002) 163.
- [18] M. Vogel, K. Hansen, A. Herlert, L. Schweikhard, *J. Phys. B.*, in press.
- [19] J. Laskin, C. Lifshitz, *J. Mass Spectrom.* 36 (2001) 459.
- [20] S. Krückeberg, G. Dietrich, K. Lützenkirchen, L. Schweikhard, C. Walther, J. Ziegler, *Int. J. Mass Spectrom. Ion Process.* 155 (1996) 141.
- [21] M. Vogel, A. Herlert, L. Schweikhard, *J. Am. Soc. Mass Spectrom.*, submitted for publication.
- [22] S. Frauendorf, *Z. Phys. D* 35 (1995) 191.
- [23] J.U. Andersen, E. Bonderup, K. Hansen, *J. Chem. Phys.* 114 (2001) 6518.
- [24] N.W. Ashcroft, N.D. Mermin, *Solid State Physics*, Holt-Saunders, Philadelphia, 1976.
- [25] L.D. Landau, E.M. Lifshitz, *Statistical Physics*, §39, 3rd ed., Pergamon Press, Oxford, 1980.
- [26] P.C. Engelking, *J. Chem. Phys.* 87 (1987) 936.
- [27] J.D. Cox, D.D. Wagman, V.A.M. Medvedev, *CODATA Key Values for Thermodynamics*, Hemisphere Publishing Corp., New York, 1984.
- [28] U. Näher, S. Bjørnholm, S. Frauendorf, F. Garcias, C. Guet, *Phys. Rep.* 285 (1997) 245.
- [29] T. Castro, R. Reifengerger, E. Choi, R.P. Andres, *Phys. Rev. B* 42 (1990) 8548.
- [30] M. Brack, *Rev. Mod. Phys.* 65 (1993) 677.
- [31] J. Zhao, Y. Luo, G. Wang, *Eur. Phys. J. D* 14 (2001) 309.
- [32] S. Erkoc, T. Yilmaz, *Physica E* 5 (1999) 1.
- [33] J. Uppenbrink, D.J. Wales, *J. Chem. Phys.* 96 (1992) 8520.
- [34] K. Michaelian, N. Rendon, I.L. Garzon, *Phys. Rev. A* 60 (1999) 2000.
- [35] Y. Xie, J.A. Blackman, *Phys. Rev. B* 64 (2001) 195115.
- [36] C. Jackschath, I. Rabin, W. Schulze, *Ber. Bunsenge. Phys. Chem.* 96 (1992) 1200.
- [37] G. Alameddine, J. Hunter, D. Cameron, M.M. Kappes, *Chem. Phys. Lett.* 192 (1992) 122.
- [38] H. Handschuh, C.-Y. Cha, P.S. Bechthold, G. Ganteför, W. Eberhardt, *J. Chem. Phys.* 102 (1995) 6406.
- [39] K.J. Taylor, C.L. Pettiette-Hall, O. Cheshnovsky, R.E. Smalley, *J. Chem. Phys.* 96 (1992) 3319.
- [40] V.A. Spasov, T.H. Lee, J.P. Maberry, K.M. Ervin, *J. Chem. Phys.* 110 (1999) 5208.